Lateral conductance of perfect and disordered dot lattices

1995 J. Phys.: Condens. Matter 7 849

(http://iopscience.iop.org/0953-8984/7/5/007)

J. Phys.: Condens. Matter 7 (1995) 849–866. Printed in the UK

Lateral conductance of perfect and disordered dot lattices

R W Tank and R B Stinchcombe

Department of Physics, Theoretical Physics, 1 Keble Road, Oxford OX1 3NP, UK

Received 10 August 1994, in final form 30 November 1994

Abstract. A theoretical treatment is given of the onset of lateral conductance in a dot lattice, which occurs as the number of electrons per dot is increased, thereby enlarging the dots until they touch. This is the threshold point between a dot and an antidot lattice. The conductance rise has been experimentally measured and we compare our predictions to those results. Two conduction mechanisms are considered in detail; band conductance in a perfect lattice and hopping conduction in a lattice with slight disorder. Both give an exponential rise of the lattice conductance with electron number. The effect of strong disorder is discussed, and using a mapping to a random resistor network it is shown to lead to a far more gradual rise in the conductance.

1. Introduction

In recent years there has been much study, both theoretical [1, 2, 3, 4, 5] and experimental [6, 7, 8, 9] of the properties of lattices of dots and antidots. These systems are usually created when the electron density of a two-dimensional electron gas (2DEG) is modulated, often by the action of an applied electrostatic potential. This potential can be fabricated in many ways, such as application of a voltage to a specially shaped gate on the surface of the semiconductor [10], or by etching a periodic pattern into this surface [11, 12].

Most commonly, the applied potential is periodic in two orthogonal directions. If it has a very large amplitude, or if the electron density is small, then the electrons will be confined to the regions around the minima of this potential. This gives a square lattice of dots, each containing just a few electrons. These dots can be studied using a variety of techniques but most commonly using capacitive [12, 13] or spectroscopic [11] measurements. Transport through a single dot, achieved via tunnelling to and from some nearby 2DEG 'leads' has also been seen [14, 15].

Suppose we now reduce the amplitude of the potential or increase the number of electrons. The minima of the potential start to fill and the dots increase in size. Eventually a point is reached where the dots just touch. We will call this *threshold*. On further increasing the electron number the 2DEG becomes connected across the entire plane. We then have a 'sea of electrons', rising out of which are the maxima of the potential. The area around each potential maximum is devoid of electrons, and is known as an antidot. Most studies of antidot lattices, whether experimental or theoretical tend to concentrate on the magnetotransport [6, 7, 8, 3, 4, 5] or spectroscopic [9, 1, 2] properties.

Consider a dot lattice just below threshold. The dots will be fairly close together, and there will be a chance for an electron to tunnel or hop from one dot to a neighbouring one, leading to a finite lattice conductivity. As the dot system gets closer to threshold this

0953-8984/95/050849+18$19.50

conductivity will increase. This onset of conductance has been seen experimentally in zero magnetic field.

A set of experiments carried out by Sundaram [16] showed this threshold behaviour very clearly. These experiments studied 2DEGs formed in a modulation doped GaAs GaAlAs heterostructure. A modulating potential was created using the ion implantation technique. The number density of the electrons was increased stepwise using the persistent photo-excitation effect, and the conductance measured at each step. The results showed a gradual rise of the conductance with electron density. The data were not complete enough to determine a functional form for the rise in conductance with electron number.

Other experiments were performed by Ismail *et al* [10]. These were carried out on a silicon MODFET which had a specially shaped gate to produce the modulating potential. The amplitude of the potential could be changed by altering the gate voltage. As the voltage was lowered from the insulating regime the rise in conductance could be measured. This time the results showed a far more rapid rise over a small change in gate voltage.

In this paper we will be concerned with the theoretical description of this onset in lateral conductance as threshold is approached. We will derive the theoretical variation of the conductance with electron number and try to explain the differences between the two experimental results.

Two different conduction mechanisms will be considered in detail; band conductance which is applicable to a lattice with very little or no disorder, and conduction via phonon assisted hopping between dots, which is applicable to a disordered lattice. In both of these mechanisms the conductance depends greatly on the shape and size of the intervening potential barrier between dots. It is therefore important to have information about the self-consistent screened potential that the electrons will feel. Additionally we will require some information about the nature of the electronic states in each dot. Before we can discuss either conduction mechanism we must address these two problems.

The outline of this paper is as follows. Section 2 outlines the calculation of the screened dot lattice potential. In section 3, the form the bound electron states in each dot will take is discussed. The band conductance of a perfect dot lattice is derived in section 4 and then section 5 treats the hopping conductance of a slightly disordered lattice. Following on from this in section 6 we discuss the effect on the conductance of a large amount of disorder in the dot lattice potential.

2. Calculating the self-consistent dot potential

As the first step we require a model for the *applied potential* which the electrons in the 2DEG then screen. This applied potential depends upon the fabrication method. We chose to model the systems used by Sundaram [16]. There, the dot lattices were created using the ion implantation technique. This uses ion damage to trap electrons in pockets lying just above the 2DEG. These trapped electrons set up a periodic electrostatic field. Correspondingly we considered a square array of charged disks, each with charge $-Q$ placed a distance h above the 2DEG. The lattice constant is a. From the experimental details presented in [16] a lattice constant of $a = 800$ nm, a disk radius $r = 300$ nm and $h = 40$ nm were used. The electron densities reported in [16] suggested that there were about 120 electrons per dot at threshold, which corresponds to a charge per disk of $Q = 1000e$.

To calculate the screened potential we used a numerical procedure, described in [17]. This is based upon the Thomas–Fermi approximation and gives us a set of self-consistent screened potentials with differing number of electrons per dot (i.e. differing chemical potentials). Some examples are shown in figure 1. The general character of the screened

potentials is that they are relatively shallow where the electron density is non-zero and rise steeply beyond the edge of the electron gas.

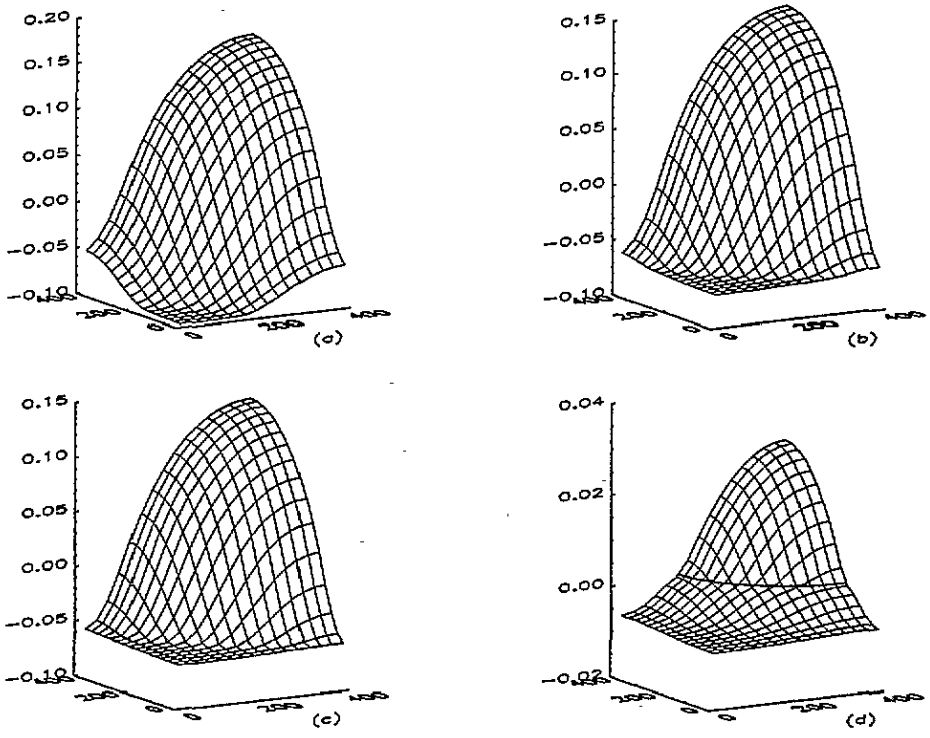

Figure 1. Three-dimensional plot of the numerically calculated screened potential for the applied potential ϕ_2. As the sequence progresses (a)–(d) the number of electrons per lattice square increases. Each plot shows only one quarter of a lattice square with lattice constant $a = 800$ nm. Defining N to be the number of electrons per lattice square and b to be a vector on the edge of the electron gas we have (a) $N = 36$, $b = (188, 0)$; (b) $N = 114$, $b = (344, 0)$; (c) $N = 168$, $b = (400, 31)$; (d) $N = 813$, $b = (400, 156)$. The contour line on plot (d) shows the edge of the electron gas. The x and y axes show distance in nm.

Although we used a very specific model for the applied potential, as discussed in [17] it is one of a class of potentials that all exhibit similar behaviour. Therefore the conclusions we draw from the conductance calculations should be applicable to other systems as well.

3. The electronic states in a single dot

Of all the states in each dot we would like to know which states are going to be important, what shape their wavefunctions take and their energy spectrum. The important states for conduction will be the highest energy bound states. With typically 120 electrons per dot at threshold it is reasonable to use semiclassical methods to study them. Although in principle a full solution can be found for any $V(x, y)$ [18] in practice this is only easy for a separable potential.

Not all of the high-energy states will be important. This is apparent when we consider the shapes of the wavefunctions. To illustrate this, consider the classical path corresponding to each WKB state. Figure 2 shows two paths for states close to the *threshold energy* (the

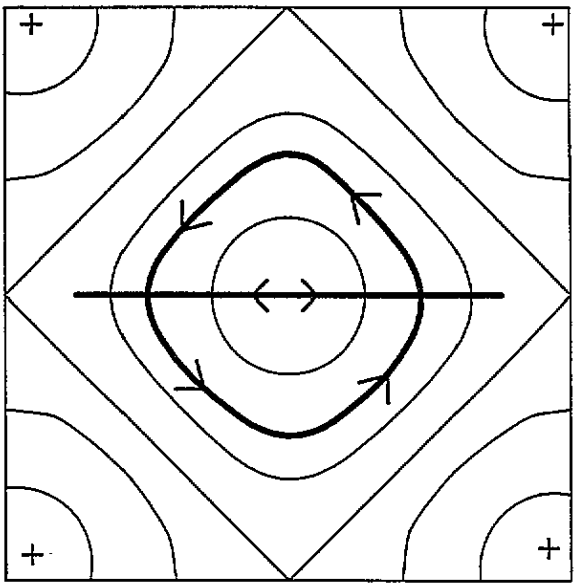

Figure 2. Contour plot of the potential of a single dot. The minimum is at the centre and the maxima of the potential lie at the corners of the square (indicated by a '+'). The heavy lines indicate classical electron paths.

energy below which all states must be bound). One path merely oscillates along the x axis. Its corresponding wavefunction is narrow in the y direction but elongated in the x direction. It will have a high probability of tunnelling to a similar state in a neighbouring dot on the x axis. The other path shown is much more circular. The wavefunction corresponding to it is more compact. It will have a very low tunnelling probability to a neighbouring dot. Such states are not important for conduction.

In general, $V(x, y)$ is non-separable and in the classical treatment of the problem there could now exist chaotic electron trajectories within each dot [19, 20]. However all realistic potentials will share some common features, such as a minimum at the origin, $\partial V/\partial y$ vanishing along the line $y = 0$, and saddle points at $(0, \pm a/2)$, $(\pm a/2, 0)$. The oscillatory orbits along the x or y axis will still be stable, and the corresponding wavefunctions will retain their elongated shape. The chaotic behaviour will affect most strongly those orbits that venture significantly in both the x and y directions. These states were however identified as not being important for conduction. Hence in our regime the chaotic dynamics can be neglected.

Now consider the energy spectrum. If the potential is separable the energy of a state will then split into 'x' and 'y' contributions; $E_{nm} = E_n^x + E_m^y$, each of which can be obtained from the Bohr quantization condition (see for example [21]) The states that are elongated in the x direction have a spectrum $E_{n1} = E_n^x + E_1^y$ where E_1^y is the lowest 1D energy. For realistic dot potentials this has a simple ladder-like form. In general $V(x, y)$ is not separable. However as the elongated states only sample the space close to one of the two axes it can be argued that the energy spectrum retains its ladder form.

As an example we applied the WKB quantization to the simple potential

$$V(x, y) = V_0 \left[\cos\left(\frac{2\pi x}{a}\right) + \cos\left(\frac{2\pi y}{a}\right) \right]$$

with $V_0 = 2.0$ meV and $a = 800$ nm. Figure 3 shows the resulting *full* energy spectrum.

The levels corresponding to the elongated states are shown with a heavy line and are replotted to the right of the spectrum. The dotted line shows the energy below which all states are bound.

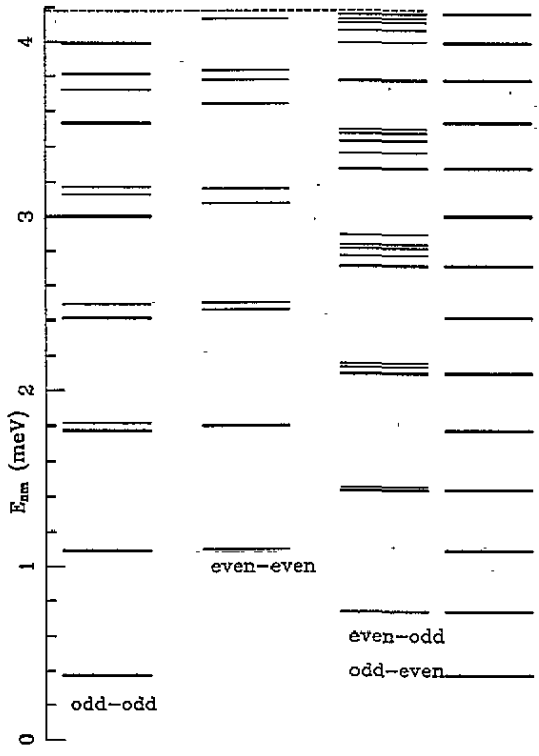

Figure 3. An example WKB energy spectrum of bound states in a single dot. The column labelled odd–odd corresponds to states where both the x and y parts of the wavefunction are even. Similar definitions apply to the other columns.

4. Band conduction in a perfect lattice

The bound states of each individual dot will be perturbed by the potential of the rest of the lattice. From the tight-binding viewpoint this leads to band formation. In this section we will calculate the expected widths of these bands and then the conductance of these bands as a function of the electron number N. In order for the tight-binding calculations to be valid the overlap between the states must be small. This assumption breaks down close to threshold.

4.1. Band formation

So long as the bandwidth is small compared to the unperturbed level spacing it will suffice to consider just one pair of degenerate states in each dot. We will denote these two base states in the dot at $\boldsymbol{R}$ by $|a_{\boldsymbol{R}}\rangle$ and $|b_{\boldsymbol{R}}\rangle$, where we will take $|a_{\boldsymbol{R}}\rangle$ to be elongated in the x direction. These states have energy E_0.

In principle we would now need to perform a *degenerate* tight-binding calculation using the sets $\{|a_{\boldsymbol{R}}\rangle\}$ and $\{|b_{\boldsymbol{R}}\rangle\}$. However simplifications can be made. Firstly the overlap

$\langle a_R|b_R\rangle = M$ will be very small and can be taken to be zero. In addition the following matrix elements will be small and can be neglected:

$$\langle a_S|(V - V_R)|b_T\rangle \qquad \langle b_S|(V - V_R)|a_T\rangle$$
$$\langle a_{S\pm\hat{y}}|(V - V_R)|a_S\rangle \qquad \langle b_{S\pm\hat{x}}|(V - V_R)|b_S\rangle.$$

Here, V is the lattice potential and V_R a dot potential. The first two are small, by virtue of the small overlap of $|a_R\rangle$ and $|b_R\rangle$. The third matrix element involves the overlap of a state $|a_R\rangle$ and an identical state located a lattice constant a away in the y direction. This overlap will be small because the state $|a_R\rangle$ is narrow in the y direction. The last matrix element is small for a similar reason. The remaining (dominant) overlaps are then

$$L = \langle a_{S\pm\hat{x}}|(V - V_R)|a_S\rangle = \langle b_{S\pm\hat{y}}|(V - V_R)|b_S\rangle$$
$$J_0 = \langle a_R|V - V_R|a_R\rangle = \langle b_R|V - V_R|b_R\rangle.$$

We are then left with two non-degenerate tight-binding calculations to perform. The results of such calculations are well known (see for example [22]) and we can immediately write the two solutions

$$E_a(k) = E_0 + J_0 + 2L\cos(k_x a) \tag{1}$$
$$E_b(k) = E_0 + J_0 + 2L\cos(k_y a). \tag{2}$$

For each of these solutions the energy depends only on one component of the wavevector k. Despite the fact that the dots are arranged on a 2D square lattice, because we neglected all mixing of the $|a_R\rangle$ and $|b_R\rangle$ states the bands that form have a 1D character. The two solutions are orthogonal to each other, and their energies overlap completely.

The higher-order corrections to this structure will involve mixing of the states and this restores a two-dimensional character. However these corrections are very small [23], and the 1D character is retained to high accuracy.

4.2. *Estimation of the bandwidth* $|4L|$

There are at least two ways of making an estimate of this integral.

Firstly, the overlap L gives a measure of the tunnelling probability of an electron through the barrier between dots. Such probabilities can also be evaluated quasiclassically [24]. For small tunnelling probabilities we obtain

$$|4L| = \frac{2}{\pi}\hbar\omega\,\mathrm{e}^{-\epsilon} \tag{3}$$

where ω is the classical frequency and the quantity ϵ is given by

$$\epsilon = \frac{1}{\hbar}\int_{x_1}^{x_2}|p|\,\mathrm{d}x = \frac{\sqrt{2m^*}}{\hbar}\int_{x_1}^{x_2}\sqrt{E + e\phi(x, y)}\,\mathrm{d}x \tag{4}$$

the integral being taken across the narrowest part of the barrier. Here E is the electron energy measured from the zero of the potential energy $(-e\phi)$.

The second method will be described in more detail later. Here we try to evaluate the integral directly and it gives the following estimate.

$$|4L| \propto (W + \lambda)\,\mathrm{e}^{-(1/\hbar)\sqrt{(2m^*H)}W} \tag{5}$$

where W is the width of the potential barrier, H is its height and λ is a distance which is small compared to a typical width W.

Both estimations fail when the barrier becomes small, and predict that the bandwidth goes to zero. The quasiclassical method breaks down for two reasons: (a) the tunnelling

probability is no longer small and equation (4) fails, and (b) the classical motion approaches a separatrix. The period diverges and the normalization of the semiclassical wavefunctions breaks down. In the second, 'direct' method, certain assumptions made when evaluating the integral fail.

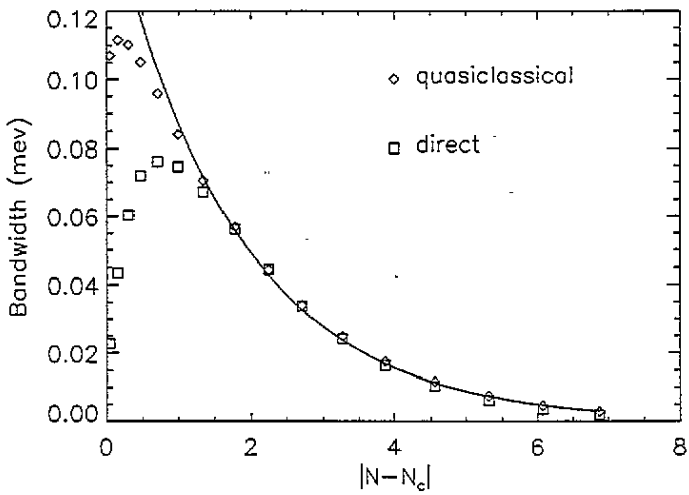

Figure 4. The tight-binding bandwidth calculated by both the quasiclassical and square-well methods. The line is $0.154\exp(-0.57|N - N_c|)$.

The results are shown in Figure 4. Both methods give exponential tails, $|4L| \propto \exp(-\alpha|N - N_c|)$, where $(N - N_c)$ is the difference between the number of electrons per dot and the number per dot at threshold. For the quasiclassical method $\alpha = 0.57 \pm 0.01$ and for the direct method $\alpha = 0.61 \pm 0.02$. This form is expected considering equations (3) and (5). Only the quasiclassical method gives an absolute value for the bandwidth and the 'direct' points have been rescaled to this amplitude.

The width of the bands is of order $0.01 \rightarrow 0.08$ meV. This is smaller than the level spacing of the elongated states, which is of order 0.15 meV, justifying the use of just one pair of basis states per dot.

4.3. The band conductance

We shall now assume the existence of a weak disordered potential created by a system of isolated randomly positioned donor impurities situated close to the 2DEG.

For a large lattice the conduction is diffuse and we can use a standard Boltzmann equation approach. The details are well known, see for example [22]. For an applied electric field ε in the x direction the current density will be

$$J_x = \frac{2e^2}{\pi\hbar}\frac{1}{a}\varepsilon \int \tau v(E)\frac{\mathrm{d}\rho}{\mathrm{d}E}\,\mathrm{d}E. \tag{6}$$

Here $\tau(E)$ the scattering time, $v(E)$ the electron velocity and ρ the Fermi–Dirac distribution function. One can show that [23] $\tau \propto v(E)$ (physically, the scattering rate should be proportional to the density of states).

The conductance due to a single band centred at energy E_n will be

$$\sigma = \sigma_0|2L|^2 \int_{E_n-|2L|}^{E_n+|2L|} \left[1 - \left(\frac{E - E_n}{|2L|}\right)^2\right]\frac{\mathrm{d}\rho}{\mathrm{d}E}\,\mathrm{d}E. \tag{7}$$

The total conductivity can be obtained by summing contributions from all the bands. At $T = 0$, the derivative of the Fermi function will be a delta function and the integral becomes

$$\sigma \propto |2L|^2 \left[1 - \left(\frac{E_F - E_n}{|2L|}\right)^2\right].$$

The conductance will therefore show oscillatory behaviour. It will be zero when E_F lies between two bands and maximum at the centre of each band. The height of the maximum is proportional to $|2L|^2$, showing an exponential increase with electron number as threshold is approached.

However all real experimental systems are at finite temperature. The typical bandwidth for our model lies in the region $0.02 \rightarrow 0.08$ meV, comparable to experimental thermal energies. In this case the width of the derivative of the Fermi function is as large or larger than the bandwidth. The conductivity will then be thermally averaged and more than one band will contribute. This leads to a smooth exponential rise

$$\sigma = \sigma_0 \, e^{-2\alpha|N - N_c|}$$

with $\alpha = 0.6$ for our system.

There is some evidence for the existence of this behaviour in the experiments by Ismail *et al* [10]. These were carried out on a MODFET device at 4.2 K in zero magnetic field. The modulation of the 2DEG was achieved by applying a voltage to a specially shaped square lattice gate on the surface of the semiconductor. The source–drain current was measured as a function of this source–gate voltage. For small changes, one would expect the change in electron number to be proportional to the change in voltage. We therefore predict that the conductance at threshold should rise exponentially with the source–gate voltage. Figure 5 shows points on an experimental curve taken from [10], on top of which is a fitted exponential curve. This system shows the predicted threshold behaviour. There are slight oscillations superimposed onto this rise. This indicates that the system is in a regime where the temperature had not yet completely smeared out the band structure oscillations.

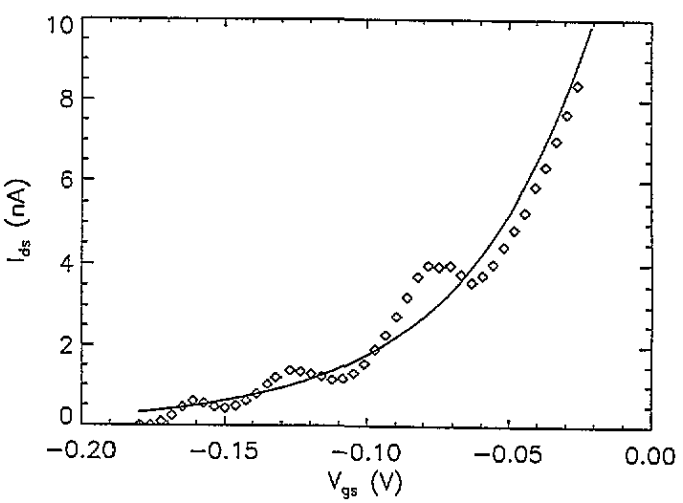

Figure 5. This shows an experimental curve taken from [10] which shows threshold behaviour. The line shows a fitted exponential curve $I_0 \exp(\kappa V_{gs})$ with $I_0 = 15.3$ nA and $\kappa = 21.5$ V^{-1}.

5. Hopping conduction in a lattice with slight disorder

The bands discussed above were very narrow, and a small amount of disorder in the screened potential will be enough to destroy their formation. A plausible mechanism for the lattice conductance would then be via hopping of electrons between bound states in neighbouring dots. In this section we will obtain an analytic expression for the dependence of the hopping rate on the parameters of the barrier and wavefunctions. We then examine the distribution that will arise for the conductances of the individual barriers, and finally relate this to the lattice conductance.

5.1. Calculation of the hopping rate

Consider two dots neighbouring in the x direction which are labelled i and j. Each will contain a bound state $\Psi_n^i(r)$ and $\Psi_m^j(r)$ with energies E_n^i and E_m^j. Again the potential of the rest of the lattice causes mixing, leading to the formation of two new states

$$\Phi^i(r) = \Psi_n^i(r) + d_j\Psi_m^j(r)$$
$$\Phi^j(r) = \Psi_m^j(r) - d_i\Psi_n^i(r).$$

Here the quantities d_i and d_j are obtained from a variational method; for example minimizing $\langle\Phi^i|H|\Phi^i\rangle/\langle\Phi^i|\Phi^i\rangle$ will give d_j. The phonon assisted hopping rate will be given by

$$W_{ij} = \frac{2\pi}{\hbar}\int |M_{ij}|^2\delta(E_j - E_i + \hbar\omega_p)\rho_{ph}\,d^3p \tag{8}$$

where $\hbar\omega_p$ and ρ_{ph} are the energy and density of states of a phonon with wavevector p. In the deformation potential approximation [25] the matrix element M_{ij} is given by

$$M_{ij} = V_1\left(\frac{\hbar}{2\rho V v_s}\right)^{1/2}|p|^{1/2}\sqrt{n_p}\langle\Phi_i|e^{ip\cdot r}|\Phi_j\rangle. \tag{9}$$

Here ρ is the density, V the volume, v_s the velocity of sound and n_p is the occupation number of a phonon state with energy $\hbar\omega_p$.

In order to proceed analytically we need to assume *trial functions* for the potential and wavefunctions. These are chosen to capture as much of the physics as possible, and yet also have a simple enough form that we can evaluate the integrals analytically. In practice this second requirement will play the strongest role in our choice.

To represent an elongated state centred at the origin we chose the form $\Psi(r) = \psi(x)\phi(y)$. Here

	Even	Odd
$x < -b$	$\psi(x) = C_1\,e^{k_1x}$	$\psi(x) = -C_1\,e^{k_1x}$
$-b < x < b$	$\psi(x) = C_2\cos(k_2x)$	$\psi(x) = C_2\sin(k_2x)$
$x > b$	$\psi(x) = C_1\,e^{-k_1x}$	$\psi(x) = C_1\,e^{-k_1x}$.

C_2 and C_1 are normalization constants. The form for the exponential decay in the classically forbidden region is a generic one, except for strongly localizing potentials (such as a quadratic potential) which are not suitable here. The natural choice for $\phi(y)$ is

$$\phi(y) = \frac{1}{\pi^{1/4}}\frac{1}{l^{1/2}}\,e^{-(y^2/2l^2)}. \tag{10}$$

This is suitable because close to the line $y = 0$ all realistic potentials will look harmonic in the y direction. For our system $l = 50$ nm. The two states $\Psi_n^l(r)$ and $\Psi_m^j(r)$ will then be specified with the parameters k_1, k_2, b_i and q_1, q_2, b_j.

Following on from the assumption that the wavefunction separates, we will assume a separable potential $V(x) + V(y)$. For a dot centred at $(a/2, 0)$ we chose

$$\begin{aligned} &0 < x < a/2 - b && V(x) = V_0\left[1 - \cos(2\pi x/a)\right] \\ &a/2 - b < x < a/2 + b && V(x) = V_0'\left[1 - \cos(2\pi x/a)\right] \\ &a/2 + b < x < a && V(x) = V_0\left[1 - \cos(2\pi x/a)\right]. \end{aligned} \tag{11}$$

Here the constant $V_0' > V_0$. Figure 6 shows the true and trial potentials for $N = 100$. The trial function does describe the barrier quite well, and we therefore hope that it will be able to capture the physics of the problem.

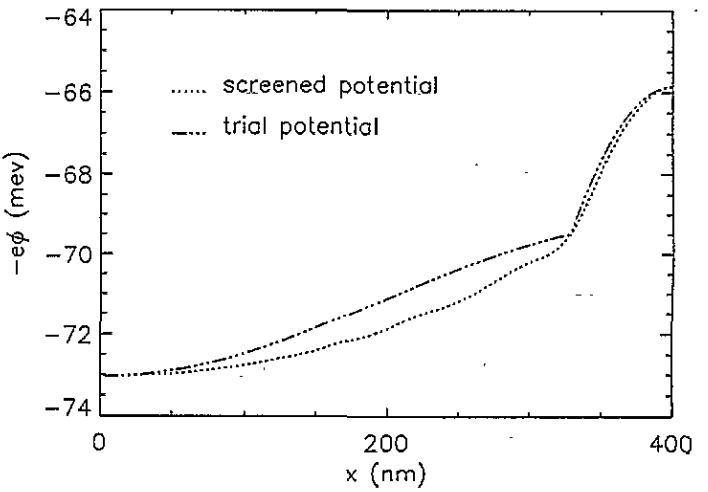

Figure 6. Cross sections of both the screened and trial potentials, taken along the x axis. The edge of the electron gas is at $x = 330$ nm.

Using these functions the integral in equation (8) becomes [23]

$$W_{ij} = W_0 V_0'(kw)^2 \, e^{-2kw} (\Delta E)^2 \, e^{-(\beta' + 1/k_B T)\Delta E}. \tag{12}$$

Here $k = (k_1 + q_1)/2$, w is the barrier width, β' is a constant which for our system has the value 14.0 ± 0.1 meV^{-1} and k_B is the Boltzmann constant. The factor W_0 is an overall undetermined constant. The factors in this expression are all physically reasonable. The factor $\exp(-2kw)$ is a typical factor for tunnelling through a barrier. It is moderated by the $(kw)^2$ term. This arose because the non-oscillatory behaviour of the wavefunctions in the barrier leads to a large contribution to the overlap integrals from this region. The $\exp(-\beta'\Delta E)$ factor reflects the reduction of the value of the matrix element as the energy difference of the two states increases. Then $(\Delta E)^2$ and $\exp(-\Delta E/k_B T)$ factors arise from the density of states and occupation number of the phonons.

When the barrier gets very small, equation (12) will fail because (a) the hopping rate is no longer small and (b) approximations required to evaluate M_{ij} fail at small k. Our calculations were for a suitable set of ranges for the parameters k and ΔE, deduced from the results in [16]. However these would be similar in other experimental systems. More importantly, the arguments given for the physical origin of the factors should apply to

other systems. Therefore, we believe that the form of (12) will capture the physics of the transition rate for this and other systems, although the exact functional form would change.

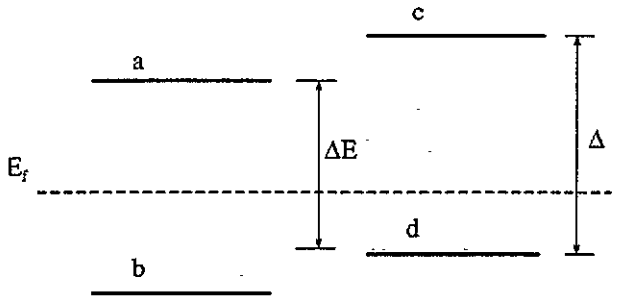

Figure 7. In each dot there will be two elongated states important for conduction. This is indicated here by the pairs *ab* and *cd*. The energy Δ is the mean level spacing of the elongated states.

5.2. The distribution of individual conductances

Consider two states a and b either side of a barrier. The conductance of the barrier due to these states will be [26]

$$\sigma_{ab} = \frac{e^2}{k_B T} f_a(1 - f_b) W_{ab}. \tag{13}$$

Here f_α is the occupancy of state α, $\alpha = a$ or b. In practice each dot will contain two states that are important for conduction. One state will lie just below the Fermi level, E_F, and one state just above E_F. This is illustrated in figure 7. In order to simplify the analysis we assume that kT is small compared to the mean level spacing Δ. Then the distribution factors (e.g. $f_a(1 - f_d)$) will be close to either zero or 1. This implies that there is little current between the pairs ac or bd, but significant current between the pairs ad or bc. The effective conductance between a dot i and a neighbouring dot j is then

$$\sigma_{ij} = \sigma_0 [W(\Delta E) + W(2\Delta - \Delta E)] \tag{14}$$

where $\Delta E = E_a - E_d$. For our system, the above simplification requires temperatures small compared to 1.7 K. Typical experimental temperatures in [16] were 0.35 → 1.5 K. So the approximation $kT \ll \Delta$ begins to fail at higher temperature.

The hopping rate W depends upon the four parameters $k, w, \delta E, V_0'$. In a disordered lattice these will all have some distribution of values. For simplicity we will take a distribution in only two, namely k and ΔE. This is not so bad because k and w always appear combined as their product and the quantity V_0' varies little with N and so would have a narrow distribution.

Consider the distribution of ΔE. A small amount of disorder will not greatly affect the level spacing, but will shift the spectra of neighbouring dots relative to each other. Thus we chose the distribution

$$P_E(\Delta E) = \begin{cases} \dfrac{1}{E_1 - E_2} & \text{for } E_1 < \Delta E < E_2 \\ P_E(\Delta E) = 0 & \text{otherwise.} \end{cases} \tag{15}$$

The upper bound is given by the mean level spacing in a single dot; $E_2 = 0.15$ meV. The lower bound arises from level splitting and is of the order of the bandwidths; $E_1 = 0.01$ meV.

The distribution of k values has no strict bounds and for simplicity we chose a Gaussian form

$$P_k(k) = \frac{1}{\delta k\sqrt{\pi}} e^{-((k-\bar{k})/\delta k)^2}. \tag{16}$$

The distribution of values of (kw) will also be Gaussian. However as $\bar{k}$ increases so will w and hence so will the width of the distribution; $w\,\delta k$. This is physically reasonable. As the electron number decreases so will the screening of both the applied and disordered potential, increasing the absolute size of the disorder.

This regime of slight disorder occurs when the width of the distribution of k is small compared to the range of k over which the conductance of a barrier will show a large rise. In our case this range is $\delta k = 0.03$ nm^{-1}. The effect of strong disorder is discussed later.

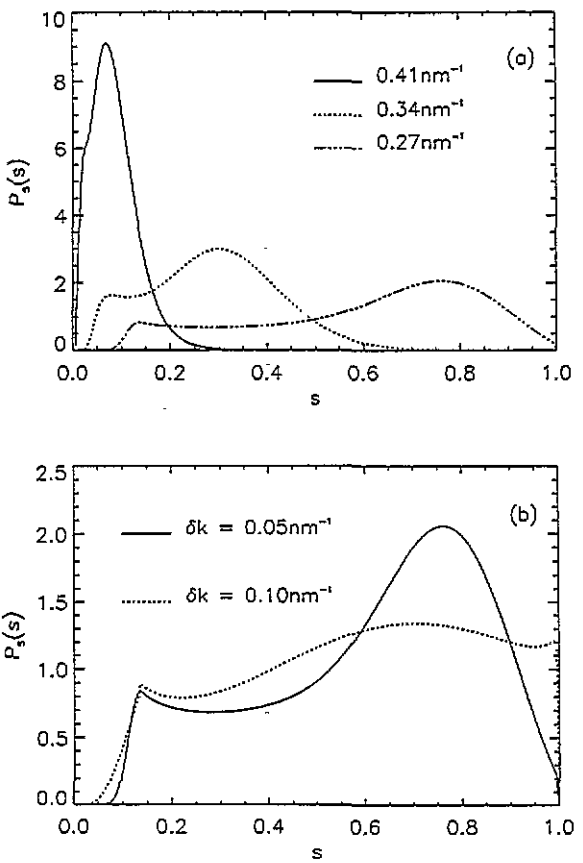

Figure 8. Some example results for the distribution $P_S(s)$. In (a) all plots have $\delta k = 0.05$ nm^{-1}. The numbers indicate the values of $\bar{k}$. In (b) both plots have $\bar{k} = 0.27$ nm^{-1}.

Given the distributions P_k, P_E and the expression (14) for a single conductance, it is fairly straightforward to calculate the distribution for σ. Figure 8 shows results for different

values of both $\bar{k}$ and δk. For clarity we plot s where

$$\sigma_{ij} = \sigma_0 \frac{V_0'}{\beta' + 1/k_B T} s(k, w, \Delta E). \tag{17}$$

The constant σ_0 is such that the maximum value of s is 1. Figure 8 shows clearly how as the electron number is increased (and $\bar{k}$ decreases) the weight of the distribution shifts to higher values, and also how an increase in the disorder leads to a wider distribution.

5.3. The lattice conductance

We can now view the dot lattice as a random resistor network. The nodes represent the dots and the links the barriers. There is a well established decimation (or real space renormalization group) procedure for treating such systems [27, 28]. This involves the repeated application of a transformation in which the four conductances round a single lattice square, $\sigma_1, \sigma_2, \sigma_3, \sigma_4$, are replaced by a single conductance σ^* across the diagonal, where from the rules for serial and parallel combination of conductances

$$\sigma^* = \frac{\sigma_1 \sigma_2}{\sigma_1 + \sigma_2} + \frac{\sigma_3 \sigma_4}{\sigma_3 + \sigma_4}. \tag{18}$$

The effect of this decimation is shown in figure 9. After repeated application the distribution for the new conductances σ^* will tend towards the distribution for the conductance of the entire lattice.

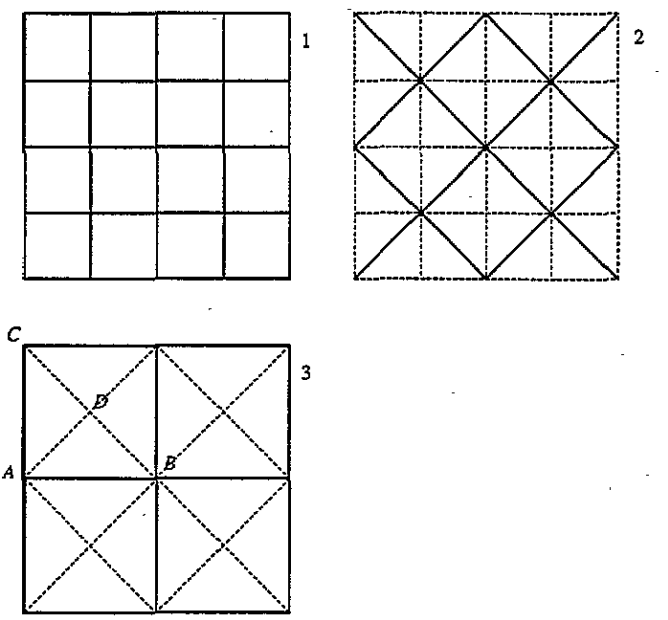

Figure 9. This shows the result on a portion of the lattice of two successive applications of the decimation procedure.

This decimation procedure is in fact only approximate as it introduces correlations between neighbouring resistors and next nearest and higher-order neighbours on the decimated lattice. For example consider the third lattice shown in figure 9. The conductances AB and AC will be correlated because the two sets of four conductances from which they

were derived both contain a common element, namely conductance AD. In general these correlations do not have a large effect [27], and we are justified in neglecting them.

In any finite system we cannot indefinitely iterate the decimation. After n iterations, the area of a lattice square will increase by a factor of 2^n. For finite size effects not to be important, the number of squares in the original lattice must be large compared to this number. In the results that follow we used at most 10 iterations, giving a factor of 1024. The experimental systems [16] contained typically 65 000 dots, allowing us to neglect the finite size.

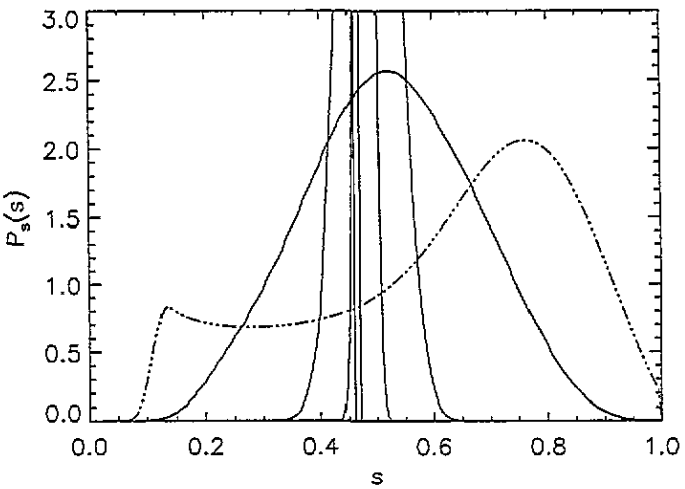

Figure 10. The results of decimation applied to the distribution with $\bar{k} = 0.27$ nm^{-1} and $\delta k = 0.05$ nm^{-1}. The plot shows the 1st, 3rd, 5th and 9th decimations. The dot-dash line shows the original distribution. The decimated distributions are shown as solid lines, becoming narrower with increasing number of the iteration.

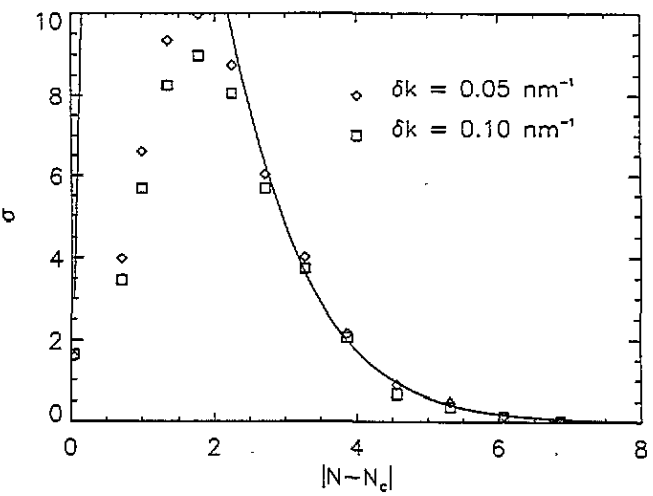

Figure 11. Variation of the conductance of a square lattice with electron number, $|N - N_c|$. The line shows the fitted curve $\sigma = \sigma_0|N - N_c| \exp(-1.31|N - N_c|)$.

In figure 10 we plot the result for one particular distribution, showing how it quickly narrows to a single value. The variation of this lattice conductance with N is shown in figure 11. The results for the two values of δk are very similar. Both curves show a downturn at small N. This is spurious, and is caused by the breakdown of equation (12) for W_{ij} for small values of k. The tail of the conductance for larger k fits well to the form

$$\sigma = \sigma_0 |N - N_c| \, e^{-\gamma |N - N_c|}$$

where the factor $\gamma = 1.31 \pm 0.04$ for $\delta k = 0.05$ and $\gamma = 1.35 \pm 0.04$ for $\delta k = 0.01$. These are comparable to the values for the exponential decay in a perfect lattice. The functional form of σ is slightly different due to the additional factor of $|N - N_c|$.

Once again the conductance rise shows a rapid increase over a small change in the electron number. While in agreement with the experiments of Ismail *et al* [10] this is in contrast to the results presented by Sundaram [16]. In the next section we will argue that this discrepancy can be resolved by the presence of a large level of disorder.

6. Conduction in the presence of strong disorder

For simplicity we assume now that the conductance of a single barrier depends upon just one variable rather than four, namely the variable k. The strongly disordered regime occurs when the width of the distribution of values of k is greater than the range of k over which the barrier conductance $\sigma(k)$ shows a large increase.

When k^2 is large the barrier is high, and when k^2 drops below zero the barrier is surmounted (the Fermi level lies above the saddle point in the potential). If the distribution of k is wide, a significant number of barriers are very high, and a significant number have been overcome. The fraction that lie in the intermediate stage will be small, because this stage covers only a small range in k. The distribution of bond conductances then shows a large peak close to zero, and close to the conductance value of a small open constriction. This approximately binary distribution is characteristic of a bond percolation problem. Correspondingly, the lattice conductance depends less on the functional form of $\sigma(k)$ and is partly governed by the percolative character of the problem.

To illustrate this we construct an approximate analytic form for $\sigma(k)$. For k^2 positive we assume the form

$$\sigma(k) = \frac{1}{e^{-\alpha k^2} + 1} \qquad \text{for } k > 0.$$

This is the well known factor for tunnelling through a one-dimensional barrier [21]. Here α can be deduced from the screened potentials. When k^2 drops below zero the two neighbouring dots will be joined by a constriction. We have not addressed the conductance of an open constriction. However as this section is illustrative we will make the unjustified assumption that the conductance is proportional to the number of states in the constriction (analogous to a point contact), which in turn we will assume is proportional to the constriction depth. This quite arbitrary choice will give

$$\sigma(k) = \beta k^2 + \tfrac{1}{2} \qquad \text{for } k < 0$$

where again the constant β can be obtained from the screened potential assuming a level spacing in the constriction of 0.1 meV.

In figure 12, we show the resulting bond conductance distribution, assuming once again a Gaussian distribution for k. As the width of the distribution increases, the conductance distribution develops a 'two peaked' structure typical of percolation conductivity [27, 28].

If $\bar{k}$ is changed for a fixed δk then there is a shift in the weight of the distribution between the peak at zero and at 0.5.

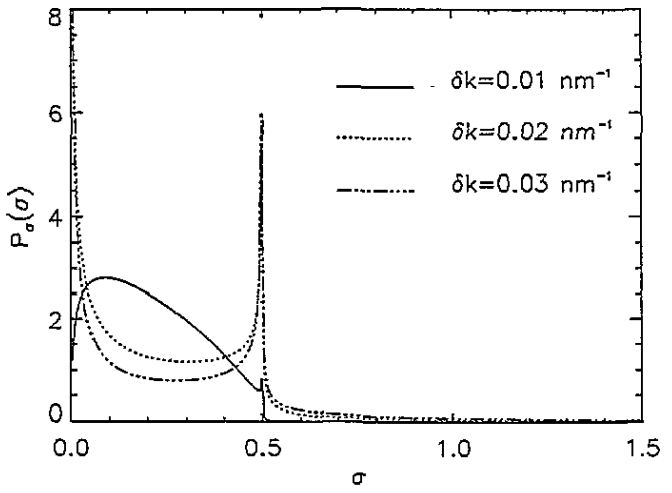

Figure 12. The conductance distribution, $P_\sigma(\sigma)$, for three different values of the width δk. All plots have $\bar{k} = 0.02$ nm^{-1}.

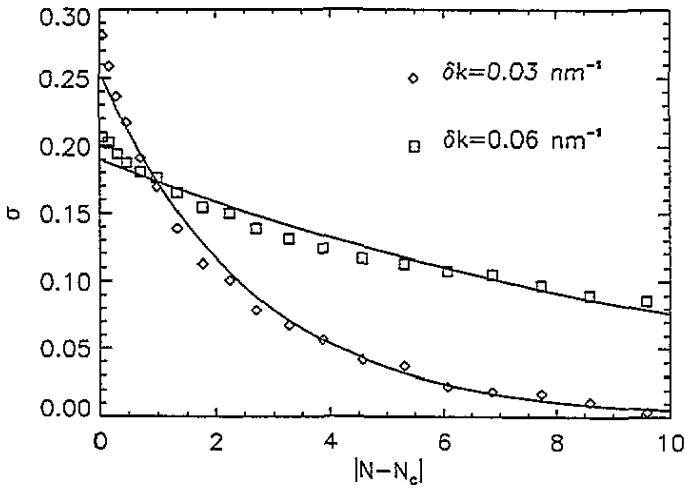

Figure 13. The lattice conductivity deduced by decimation, plotted as a function of the difference between the number of electrons per dot at threshold and the mean number of electrons per dot. The lines show fitted exponentials.

Applying the decimation procedure gives the lattice conductance shown in figure 13. As the magnitude of the disorder increases the conductance rise becomes slower. We can attempt to again fit an exponential form $\sigma \propto \exp(-\gamma|N - N_c|)$ to the data values for the conductance, giving $\gamma = 0.39 \pm 0.01$ for $\delta k = 0.03$ nm^{-1} and 0.091 ± 0.004 for $\delta k = 0.06$ nm^{-1}. These values are dramatically lower than the exponents for a weakly disordered or perfect lattice, and the fit is poorer. Returning to the experimental results presented by Sundaram [16], we can now see that the slow rise in conductance observed is an indication of a significant level of disorder in the dot lattices studied.

7. Conclusions

In this paper we considered the onset of conductance in a dot lattice as it approaches threshold with an antidot lattice. At any one point the transport through the lattice depends greatly on the size of the potential barrier between dots. It was therefore important to quantify the dimensions of this barrier and the manner in which it changes with changing electron number. We also required information about the wavefunctions of the dot states that are important for conduction. We argued that, for a dot with sufficient number of electrons, these states have a highly elongated shape, extended along one axis of the lattice and narrow along the direction of the other axis. Their energy spectrum is ladder-like. Whereas chaotic orbits will exist within a dot, these will not play an important role in the conduction process. This is in contrast to the case for an antidot lattice, where the chaotic orbits are very important [3, 29].

Using these results we calculated the lateral conductance of a dot lattice in zero magnetic field. We considered two cases, namely that of a perfect lattice and that of a lattice with slight disorder. Corresponding to these two cases we had two different conduction mechanisms. For the first we considered the band conductance of a tightly bound band, and for the second conduction via phonon-assisted hopping of electrons between neighbouring dots. The variation in conductance with increasing electron number was calculated.

Both mechanisms gave similar results. This is not so surprising as in essence they both depended greatly on the variation with electron number of the ease of tunnelling through the barrier between neighbouring dots. As threshold is approached there is a large increase in the conductance over a small change in the electron number. The tail of the conductance rise was exponential in character. For our system the region in which the conductance turned on encompassed a total change in the mean electron number per dot of 8. This corresponds to a fractional change of 0.07. Such a dramatic rise over a short range has been seen in experiments by Ismail *et al* [10]. However in the experiments by Sundaram [16] the rise in conductance occurred over a far larger change in electron number.

In the last section we showed that this discrepancy could be explained by a strong level of disorder being present in the systems studied in [16]. This is plausible considering the differing fabrication processes. A lithographic technique was used in [10], with which it is relatively easy to accurately define a periodic gate. In contrast it is harder to accurately position the ion beam used in [16] to produce the patterning.

With the increasing advances in lithographic techniques it is becoming easier to produce systems with less and less disorder. If the system is such that it can be swept from a dot to an antidot lattice then it should exhibit the threshold phenomena discussed in this paper. The rapidity of the conductance rise at threshold will be a good experimental indication of the level of disorder in the system potential.

References

[1] Que Wei-ming and Kirczenow G 1988 *Phys. Rev.* B **38** 3624
[2] Wu G Y and Zhao Y 1993 *Phys. Rev. Lett.* **71** 2114
[3] Fleischmann R, Geisel T and Ketzmerick R 1992 *Phys. Rev.* B **68** 1367
[4] Tan Yong 1994 *Phys. Rev.* B **49** 1827
[5] Oakeshott R B S and MacKinnon A 1993 *J. Phys.: Condens. Matter* **5** 6991
[6] Lorke A, Kotthaus J P and Ploog K 1991 *Phys. Rev.* B **44** 3447
[7] Weiss D, Roukes M L, Menschig A, Grambow P, von Klitzing K and Weimann G 1991 *Phys. Rev. Lett.* **66** 2790
[8] Paris E, Ma J, Kriman A M, Ferry D K and Barbier E 1991 *J. Phys.: Condens. Matter* **3** 6605

[9] Lorke A, Kotthaus J P and Ploog K 1990 *Phys. Rev. Lett.* **64** 2559
[10] Ismail K, Chu W, Yen A, Antoniadis D A and Smith H I 1989 *Appl. Phys. Lett.* **54** 460
[11] Sikorski Ch and Merkt U 1989 *Phys. Rev. Lett.* **62** 2164
[12] Smith III T P, Lee K Y, Knoedler C M, Hong J M and Kern D P 1988 *Phys. Rev.* B **38** 2172
[13] Hansen W, Smith III T P, Lee K Y, Brum J A, Knoedler C M, Hong J M and Kern D P 1989 *Phys. Rev. Lett.* **62** 2168
[14] Reed M A, Randall J N, Aggarmal R J, Matyi R J, Moore T M and Wetsel A E 1988 *Phys. Rev. Lett.* **60** 535
[15] Weis J, Hang R J, von Klitzing K and Ploog K 1993 *Phys. Rev. Lett.* **71** 4019
[16] Sundaram G 1992 *DPhil Thesis* Oxford University
[17] Tank R W and Stinchcombe R B 1994 *J. Phys.: Condens. Matter* **6** 5007
[18] Gutzwiller M C 1990 *Chaos in Classical and Quantum Mechanics* (Berlin: Springer)
[19] Geisel T, Zacherl A and Radons G 1987 *Phys. Rev. Lett.* **59** 2503
[20] Geisel T, Zacherl A and Radons G 1988 *Z. Phys.* B **71** 117
[21] Landau L D and Lifshitz E M 1977 *Quantum Mechanics* 3rd edn (New York: Pergamon)
[22] Peierls R E 1955 *Quantum Theory of Solids* (Oxford: Clarendon)
[23] Tank R W 1994 *DPhil Thesis* Oxford University
[24] Kapur P L and Peierls R E 1937 *Proc. R. Soc.* A **163** 606
[25] Kittel C 1987 *Quantum Theory of Solids* (Chichester: Wiley)
[26] Miller A and Abrahams E 1960 *Phys. Rev.* **120** 745
[27] Stinchcombe R B and Watson B P 1976 *J. Phys. C: Solid State Phys.* **9** 3221
[28] Yeomans J M and Stinchcombe R B 1978 *J. Phys. C: Solid State Phys.* **11** 4095
[29] Weiss D, Richter K, Menschig A, Bergmann R, Schweizer H, von Klitzing K and Weimann G 1993 *Phys. Rev. Lett.* **70** 4118